Longitudinal Study by 2D-Speckle-Tracking Echocardiography of the Left Ventricle Rotational Mechanics During Postnatal Adaptation in Healthy Newborns

Short title: BABYSTRAIN

Johanne Auriau*[1,2], Ba Luu Truong[1,2], Stéphanie Douchin[1], Hélène Bouvaist[1], Gabrielle Michalowicz[2], Yves Usson[2] and Pierre-Simon Jouk[2,3].

[1] Department of Cardiology, University Hospital of Grenoble and Grenoble Alpes University, CS 10217, 38043 Grenoble, France

[2] DyCTim Team, TIMC-IMAG Laboratory, 38706, La Tronche Cedex, France

[3] Department of Genetic, University Hospital of Grenoble and Grenoble Alpes University, CS 10217, 38043 Grenoble, France

* Corresponding author. Department of Cardiology, Grenoble Alpes University Hospital, CS 10217, 38043 Grenoble, France. Tel: +33-476769495. E-mail: JAuriau@chu-grenoble.fr

Relationship with the Industry: None

Funding: Financial support was provided by the University Grenoble Alpes Hospital, Department of Cardiology

Word count: 4336

Abstract

Aims: Major hemodynamic changes occurring during postnatal adaptation period lead to parietal remodeling, and modifications of ventricular mechanical constraints. The aim of this study was to compare Left Ventricular (LV) rotation parameters in healthy newborns at birth, and at their 3rd month of life, using 2D-speckle-tracking echocardiography (2D-STE).

Methods: This was a prospective, longitudinal and monocentric study conducted in healthy and full-term newborns at the Grenoble-Alpes University Hospital. Two echocardiographic assessments were successively performed: the first within the first days after birth (days 2-5); the second during the third month of life. Different LV rotation and deformation parameters were compared between examinations using 2D-STE: LV basal and apical rotation (°), LV twist (°), LV torsion (°/cm), LV untwist rate (°/s), circumferential strain (%) and radial Strain (%).

Results: 43 babies were included and 35 (82%) completed the two assessments. During the first 3 months of life, both LV twist and LV torsion increased, respectively from 4.06 ±2.18° to 8.59 ±2.66° ($p<0.001$), and from 1.34 ±0.71°/cm to 2.34 ±0.80°/cm ($p<0.001$). This difference was due to a significant increase in basal clockwise rotation from -1.99 ±1.40° to -5.63 ±1.33° ($p<0.001$), whereas there was no difference between the two apical rotation measurements ($p=0.63$). Peak values for untwist rate doubled from -48.48 ±23°/sec to -98.87 ±47.28°/sec, ($p<.001$).

Conclusions: The LV twist significantly increased during postnatal adaptation period, mainly explained by a radical change in LV basal rotation. Parallelly, the LV peak untwist rate considerably increased, playing a part in the improvement of LV diastolic function in neonates. We introduce a new tissular perspective of the LV diastolic function improvement in neonates, namely: the progressive onset of the LV twist subsequent to the ventricular remodeling that occurred after the drop of pulmonary and right ventricular pressures.

Keywords: Healthy newborns, LV twist, LV Rotation, Postnatal adaptation, 2D-STE

Clinical Trial Registration: https://clinicaltrials.gov/ct2/show/NCT03654430

Introduction

Permanent progress in cardiac function assessment led to a better understanding of the different mechanisms involved in the normal left ventricular (LV) function. Hence, it has been demonstrated that during systole and diastole, the base and the apex of the LV rotate in opposite directions.[1,2] While the base rotates clockwise along the longitudinal axis of the LV when viewed from the apex, the apex rotates counter-clockwise. The twist is the net apex-to-base rotation difference and refers to the ventricular wringing motion during systole, whereas the untwist expresses the return of cardiac shape to its initial resting position during diastole.[3,4]

2D-speckle-tracking echocardiography (2D-STE) is one of the approved methods to assess rotational mechanics of the heart.[5,6] Based on the measurement of myocardial deformation by speckle tracking (natural acoustic markers), it allows rapid, non-invasive and quantitative assessment of the myocardial function and contractility.[7-9]

The post-natal adaptation period is characterized by major hemodynamic changes with the drop of right ventricular (RV) pressure, leading to parietal stress variations and parietal remodeling. Different models of helical layer architecture of the LV have been proposed to explain this mechanism, all involving the complex orientation of helical and circular muscle fibers of the LV.[10-12] Recent works focused on the analysis of the orientation of “myocardial fibers” in fetal and neonatal hearts using polarized light imaging. They showed an inhomogeneous secondary arrangement of myocardial cells after birth, especially during the first three months of life. It appears in the ventricular walls a thin area of high isotropy that could be a slippage plane between 2 highly anisotropic cardiomyocyte areas.[13-15]

Thus, we hypothesized that the onset of the left ventricle twist mechanism occurred during the postnatal adaptation period, in healthy newborns. The understanding of this physiological and adaptive mechanisms is a prerequisite to optimize therapeutic management in pathological situations.

Methods

Study population and study protocol

This was a prospective, observational, longitudinal, and monocentric study. All newborns hospitalized in the Mother and Baby Unit of the Grenoble Alpes University Hospital during April to June 2018 were prospectively screened. Inclusion criteria were: 24- to 120-hour-old newborn; birth after 37 weeks gestation; birth weight between 3rd and 97th percentile according to France sex and gestational age-specific reference data; absence of cardiac or extra-cardiac malformations at the antenatal screen; absence of maternal diabetes (gestational or mellitus); informed consent obtained by both parents.

In order to obtain high parental adhesion and few lost to follow-up, the study design was limited to two echographic assessments: the first between day 2 and day 5 of life (before discharge to home); the second between day 60 and day 90 of life. Exclusion criteria was the presence of cardiac malformation at the first echocardiography, except a small Patent Foramen Ovale (PFO) or a restrictive Patent Ductus Arteriosus (PDA). Demographic and clinical data were collected: sex, gestational age, weight, occipital frontal circumference (OFC), height, presence of cardiac murmur at auscultation, presence of bilateral femoral pulse, heart rate.

The study protocol was approved by the Committee for the Protection of Persons and a parental written informed consent was obtained before the first examination. Financial support was provided by the University Grenoble Alpes Hospital, and the study was registered on ClinicalTrials.gov (NCT 03654430).

Definitions

Left ventricular (LV) rotation refers to the circular movement of a short-axis section of LV as viewed from the apex along the long axis of LV (Figure 1). Considering radial lines connecting the center of mass to a specific point in the myocardial wall, LV rotation is defined as the angle between line position at two different times: at the end of diastole and at any time during

systole. By convention, when viewed from the apex, counterclockwise rotation is a positive value whereas clockwise rotation is a negative value.

LV twist is defined as the net difference in degrees between LV apical rotation and LV basal rotation during a cardiac cycle: LV twist (°) = LV apical rotation (°) – LV basal rotation (°). LV twist rate is the velocity at which twist occurs per unit time (degrees per second). Peak LV twist rate and peak LV untwist rate represents peak positive and peak negative velocities, respectively. LV torsion is the net LV twist angle normalized by the LV end-diastolic length and expressed in degrees per centimeter.

LV circumferential and radial strain describe the myocardial deformation normalized to its original shape and size during the cardiac cycle. While the circumferential component is tangential to the endocardial border and refers to a positive value when the LV rotates counterclockwise, the radial component is perpendicular to the endocardial border and refers to a positive value when directed towards the cavity.[16]

Objectives and endpoints

The main objective was to compare LV twist mechanism in healthy newborns at birth and at their third month of life, using the peak LV twist as primary endpoint. Secondarily, we compared other LV rotation and deformation parameters during the same period: peak LV torsion, peak LV twist rate, peak LV untwist rate, circumferential strain and radial strain. Finally, we compared the endo- and epicardial LV deformation, using the inner and outer circumferential strain as endpoints.

2D Echocardiographic imaging

All newborns were investigated in a silent, warm and dark room, lying quietly and after feeding. No sedation drugs were used. Images were obtained with a Toshiba APLIO 400 echocardiographic scanner operated by one experienced practitioner, using a (Canon Medical systems Europe B.V., Netherlands) with a 5 MHz probe (PST-50BT). Gray scale images and digital loops were acquired and stored as raw Digital Imaging and Communication in Medicine

data (DICOM) for later off-line analysis. A standard diagnostic echocardiographic assessment was performed in all newborns according to the Echocardiographic European Society recommendations.[17] For each examination, digital loops of parasternal short-axis views and apical four-chambers views were acquired including three heart cycles each. The basal plane was defined as the mitral valve leaflets plane and the apical plane was defined as the furthest apical extent of the LV cavity distal to the papillary muscles. Imaging depth of focus and width were adjusted and all images were acquired with a 2D-probe instead of a 3D-probe, in order to obtain high frame rates and better resolution, as recommended in pediatric population. LV length was determined by the distance between the midpoint of the mitral valve annulus and the LV apex in apical four-chambers view at end-diastole.

2D-speckle-tracking analysis

Offline 2D speckle-tracking analysis was performed using a dedicated software (Ultra Extend; Toshiba Medical Systems). Best quality images were selected for analysis, with the most circular shaped short-axis cross-section. When image quality was not acceptable, no analysis was done.

Three points of interest were first placed along the LV endocardium to initiate automated tracking. Then, tracking was manually adjusted to the endocardial border and myocardial thickness before starting analysis. Visual assessment of tracking adequacy was reviewed by the operator until optimal tracking was obtained (Figure 2). The software automatically divided the myocardium into six segments for basal short-axis plane (anterior; lateral; posterior; inferior; septal; antero-septal), four segments for apical short-axis planes (anterior; lateral; inferior; septal) and six segments for apical four-chambers planes (basal-lateral; mid-lateral; anterolateral; anteroseptal; mid-septal; basal-septal). The myocardium thickness was also automatically divided into two layers by the software. The inner layer was the layer between endocardium and mid-wall whereas the outer layer was the layer between mid-wall and epicardium. The mean values of both inner and outer layers were used for analyses except

when specified. No measurements of LV longitudinal strain were performed, because of many noisy images caused by the lung in 4C-apical view.

Reproducibility

Intra-observer and inter-observer reproducibility were assessed by two operators for basal rotation, apical rotation, basal circumferential strain and apical circumferential strain. The first fifteen examinations were selected for the analysis. One operator assessed intra-observer variability by performing a second off-line analysis of the same patient, one month after the first one in order to reduce recall bias. For inter-observer variability assessment, a second experienced operator analyzed the same patients blinded to the results of the first observer.

Statistical analysis

All statistical analyses were performed with JASP (version 9.0), a statistical program based on the R-Core. Standard descriptive statistics were calculated. Continuous variables were expressed as mean and standard deviation (SD), with paired *Student's t* test to compare differences between groups. Categorical variables were expressed as counts and percentage with *Fischer's* exact test to compare differences between groups. Correlations between variables were tested using the Pearson correlation coefficient. To assess intra and inter-observer variability, the intraclass correlation coefficient was calculated. In addition, data were examined by a Bland-Altman analysis. The bias was expressed as the mean difference between the two measurements, and the limits of agreement (LOA) as ±1.96 SD of the bias. To compare the timing of rotation, twist, torsion, and twist rate in relation to the events of the cardiac cycle in newborns with varying heart rates, we adjusted the cardiac cycle length to a similar scale (percentages of cardiac cycle), divided in 100 measurements using cubic interpolations. For all significance testing, a difference was considered significant at $p<0.01$.

Results

Patient characteristics and echocardiography assessment

From April to June 2018, 43 babies were included and had a first echocardiography before discharge to home. Patient characteristics and echographic parameters are reported in Table 1. Twenty-two babies (51%) out of 43 were females. No cardiac malformation was found and no patient was excluded. They were 3.44 days old (±0.77) at the first exam, weighed 3.44kg (±0.36) and measured 51cm (±2.3). Thirty-six (84%) patients out of 43 had a second echocardiography, and 7 (6%) were lost for follow-up. Mean age at the second exam was 78 days (±7.6). Due to a higher sleep state of babies at the first exam, the mean heart rate was lower compared to the second exam (112 bpm vs 150 bpm; $p<0.001$). Mean frame rates were similar between short-axis basal and apical planes at the same echocardiography. However, mean frame rates were lower at the second echocardiography compared to the first one (90Hz vs 110Hz; $p<0.001$). This difference was a consequence of the necessary extension of acquisition windows at the second exam, due to the chest and the heart growth.

Evolution of LV rotation and deformation parameters

The comparison of multiple LV rotation and deformation parameters between birth (day 2-5 of life) and third month of life in healthy newborns are presented in Table 2 and Figure 3. LV peak twist significantly increased from 4.1 ±2.2° to 8.6 ±2.7° ($p<0.001$), such as LV peak torsion from 1.3 ±0.7°/cm to 2.3 ±0.8°/cm ($p<0.001$). Although LV twist is the net difference between apical and basal rotation, there was no statistical difference between the two apical rotation measurements ($p=0.63$). Only basal rotation significantly decreased from -2.0 ±1.4° to -5.6 ±1.3° ($p<0.001$). These observations are also illustrated in Figure 4 in which mean basal rotation, mean apical rotation and mean LV twist are compared between both echocardiographies.

Similarly, there was no statistical difference between the two apical circumferential strain measurements ($p=0.12$), while basal circumferential strain was lower at the second exam

(p<0.001). Basal and apical radial strain increased between the two exams (respectively from 12.9 ±4.9% to 17.0 ±9.2% and from 14.7 ±4.6% to 27.6 ±11.1%) but a statistical difference was only demonstrated for apical plane.

Peak values for twist rate and untwist rate doubled from 41.4 ±20.4°/sec to 81.3 ±29.4°/sec and from -48.5 ±23.0°/sec to -98.9 ±47.3°/sec, respectively (p<0.001). More importantly, the mean twist rate curve morphology changed a lot between the two assessments, especially regarding the untwist rate (Figure 4). Indeed, the untwist rate peak was significantly pronounced at third month of life whereas it was difficult to depict it at birth.

Correlations between cardiac frequency and LV rotation were systematically tested. No significant correlations were found between basal rotation and cardiac frequency at both assessments. For apical rotation, a significant positive correlation was found only at the 2nd examination, during the third month of life (p<0.001). However, the Pearson correlation coefficient was very low, and only 18% of the total variance can be attributed to the positive regression between cardiac frequency and apical rotation.

Endocardial versus Epicardial LV deformation

Comparison between endocardial and epicardial circumferential strain measurements are presented in Table 3. All endocardial measurements (inner layer) were significantly more negative than epicardial measurements (outer layer). Thus, endocardial circumferential LV deformation was significantly higher than epicardial circumferential LV deformation. This difference between endocardial and epicardial layers was also demonstrated for other LV deformation parameters such as basal rotation, apical rotation, LV twist (data not shown). For rotational measurements, endocardial and epicardial layers always rotated in the same direction.

Feasibility of 2D-STE and Variability assessment

For the first echocardiography, only one 2D-STE analysis was not feasible out of 43 exams (patient 24). Indeed, the newborn was restless, and short-axis apical images were of too poor

quality for 2D-STE analysis. For the second echocardiography, all images from the 36 babies were of sufficient quality to perform a 2D-STE analysis in short axis views. However, as we excluded the patient 24 for the first 2D-STE analysis, a total of 35 (82%) patients had both 2D-STE analysis.

Intra-observer and inter-observer variability data are shown in Table 4. Intraclass correlation coefficients demonstrated good inter-observer and intra-observer measurements reliability as they were all superior to 0.85 for each parameter, even if, as expected intra-observer reproducibility was slightly better than inter-observer reproducibility.

Discussion

Our results demonstrate that LV basal rotation is very weak in early neonatal period and becomes significant three months later. This increase in clockwise basal rotation is mainly responsible for the LV twist. To our knowledge, this study is the first having analyzed the changes in LV rotational mechanics during the first months of postnatal life, that is the period of postnatal hemodynamic adaptation and myocardial modeling.

Comparison with other studies must be done according to age. In a study performed in very preterm infants (less than 29 weeks gestation), three examinations were successively performed: the first at day 1, the second at day 2 and the third between day 5 and 7 after birth.[18] Although they focused on a preterm population, their results are concordant with the results of our first examination, that is performed between their second and their third examination. It sharpens the temporal description of basal rotation during the early neonatal period; namely, the mean basal rotation was very weak and positive at both first and second exams, and became slightly negative at the third exam. Thus, we can assume that the main change in basal rotation occurs within the first weeks after birth. This suggests that it would be independent of birth term, reinforcing an adaptative mechanism due to the drop of pulmonary pressures.

Many more studies have been conducted in older children (over three years old) and adults. The overall pattern they described is similar to what we describe at second examination during the third month of life. Although peak basal rotation values can be slightly different among studies (depending on multiple factors such as the age or the software used for the 2D-STE analysis), the basal rotation profile was constant.[19-21] This reinforce our preceding assumption that main changes in basal rotation occurs during postnatal adaptation period and that the basal rotation is largely responsible for the LV twist onset. Among these studies, one analyzes the correlation between LV rotation and the increase in cardiac frequency due to exercise in children.[22] Their results showed only a positive correlation with the apical rotation and the cardiac frequency. In our study the same trends were observed, namely the changes in basal rotation were independent of the increase in cardiac frequency.

Besides those findings, we also demonstrated an important change of the untwist rate between both assessments. While the peak untwist rate was almost undetectable at the first exam, it became highly pronounced at the second exam (Figure 4). As the untwist deformation occurs in diastole and contributes to the filling of the LV by a mechanism of suction, the peak untwist rate is used as a parameter to approach LV diastolic function.[23,24] The radical increase of the untwist rate on the third month of life pleads for a LV diastolic function improvement during this period concomitantly to the remodeling of myocardial fibers that facilitates the LV twist and untwist. Although the poor diastolic function in neonates was commonly explained by cellular and molecular immaturity mechanisms, we introduce a new tissular perspective, namely: the progressive onset of the LV twist subsequent to the ventricular remodeling that occurred after the drop of pulmonary and right ventricular pressures.[25]

Conclusion

This study highlighted the evolution of different LV rotation parameters during postnatal adaptation in healthy newborns with the use of 2D-STE. We showed a radical change in LV

basal rotation leading to an increase of the LV twist. In parallel, we demonstrated a considerable increase of the LV untwist, which probably plays a main part in the improvement of LV diastolic function in neonates. All these results strengthen the assumption of a central role of the LV base mechanics during postnatal adaptation period.

References

1. Buckberg GD, Weisfeldt ML, Ballester M, Beyar R, Burkhoff D, Coghlan HC, et al. Left ventricular form and function: scientific priorities and strategic planning for development of new views of disease. *Circulation*. 2004 Oct 5;110:e333-6
2. Sengupta PP, Korinek J, Belohlavek M, Narula J, Vannan MA, Jahangir A, et al. Left Ventricular Structure and Function. Basic Science for Cardiac Imaging. *J Am Coll Cardiol.* 2006 Nov 21;48:1988-2001.
3. Burns AT, McDonald IG, Thomas JD, MacIsaac A, Prior D. Doin' the twist: New tools for an old concept of myocardial function. *Heart. 2008;94:*978–983. https://doi.org/10.1136/hrt.2007.120410
4. Sengupta PP, Tajik AJ, Chandrasekaran K, Khandheria BK. Twist Mechanics of the Left Ventricle. Principles and Application. *JACC Cardiovasc Imaging*. 2008 May;1(3):366-76. doi: 10.1016/j.jcmg.2008.02.006
5. Leitman M, Lysyansky P, Sidenko S, Shir V, Peleg E, Binenbaum M, et al. Two-dimensional strain-a novel software for real-time quantitative echocardiographic assessment of myocardial function. *J Am Soc Echocardiogr*. 2004 Oct;17:1021-9
6. Nishikage T, Nakai H, Mor-Avi V, Lang RM, Salgo IS, Settlemier SH, et al. Quantitative assessment of left ventricular volume and ejection fraction using two-dimensional speckle tracking echocardiography. *Eur J Echocardiogr*. 2009 Jan;10:82-8. doi: 10.1093/ejechocard/jen166
7. Hayabuchi Y, Sakata M, Kagami S. Assessment of two-component ventricular septum: Functional differences in systolic deformation and rotation assessed by speckle tracking imaging. *Echocardiography*. 2014 Aug;31:815-24. doi: 10.1111/echo.12484
8. Opdahl A, Helle-Valle T, Skulstad H, Smiseth OA. Strain, strain rate, torsion, and twist: echocardiographic evaluation. *Curr Cardiol Rep*. 2015 Mar;17:568. doi: 10.1007/s11886-015-0568-x

9. Stöhr EJ, Shave RE, Baggish AL, Weiner RB. Left ventricular twist mechanics in the context of normal physiology and cardiovascular disease: a review of studies using speckle tracking echocardiography. *Am J Physiol Heart Circ Physiol*. 2016 Sep 1;311:H633-44. doi: 10.1152/ajpheart.00104.2016
10. Taber LA, Yang M, Podszus WW. Mechanics of ventricular torsion. *J Biomech* 1996;29:745–52.
11. Jouk PS, Usson Y, Michalowicz G, Grossi L. Three-dimensional cartography of the pattern of the myofibres in the second trimester fetal human heart. *Anat Embryol (Berl)*. 2000 Aug;202:103-18
12. Buckberg G, Hoffman JI, Mahajan A, Saleh S, Coghlan C. Cardiac mechanics revisited: the relationship of cardiac architecture to ventricular function. Circulation. 2008 Dec 9;118:2571-87. doi: 10.1161/CIRCULATIONAHA.107.754424.
13. Jouk PS, Truong BL, Michalowicz G, Usson Y. Postnatal myocardium remodelling generates inhomogeneity in the architecture of the ventricular mass. *Surg Radiol Anat*. 2017 Nov 28
14. Desrosiers PA, Michalowicz G, Jouk PS, Usson Y, Zhu Y. Study of myocardial cell inhomogeneity of the human heart: Simulation and validation using polarized light imaging. *Med Phys*. 2016 May;43:2273. doi: 10.1118/1.4945272.
15. Yang F, Zhu YM, Michalowicz G, Jouk PS, Fanton L, Viallon M, et al. Quantitative comparison of human myocardial fiber orientations derived from DTI and polarized light imaging. *Phys Med Biol*. 2018 Oct 23;63:215003. doi: 10.1088/1361-6560/aae514.
16. Voigt JU, Pedrizzetti G, Lysyansky P, Marwick TH, Houle H, Baumann R, et al. Definitions for a common standard for 2D speckle tracking echocardiography: consensus document of the EACVI/ASE/Industry Task Force to standardize deformation imaging. *Eur Heart J* Cardiovasc Imaging. 2015 Jan;16:1-11. doi: 10.1093/ehjci/jeu184
17. Baumgartner H, Bonhoeffer P, De Groot NM, de Haan F, Deanfield JE, Galie N, et al. Task Force on the Management of Grown-up Congenital Heart Disease of the

European Society of Cardiology (ESC); Association for European Paediatric Cardiology (AEPC); ESC Committee for Practice Guidelines (CPG). ESC Guidelines for the management of grown-up congenital heart disease (new version 2010). *Eur Heart J*. 2010 Dec;31:2915-57. doi: 10.1093/eurheartj/ehq249. Epub 2010 Aug 27

18. James A, Corcoran JD, Mertens L, Franklin O, El-Khuffash A. Left Ventricular Rotational Mechanics in Preterm Infants Less Than 29 Weeks' Gestation over the First Week After Birth. J Am Soc Echocardiogr. 2015 Jul;28:808-17.e1. doi: 10.1016/j.echo.2015.02.015
19. Notomi Y, Lysyansky P, Setser RM, Shiota T, Popović ZB, Martin-Miklovic MG,et al. Measurement of ventricular torsion by two-dimensional ultrasound speckle tracking imaging. *J Am Coll Cardiol*. 2005 Jun 21;45:2034-41.
20. Takahashi K, Al Naami G, Thompson R, Inage A, Mackie AS, Smallhorn JF. Normal Rotational, Torsion and Untwisting Data in Children, Adolescents and Young Adults. *J Am Soc Echocardiogr.* 2010 Mar;23:286-93. doi: 10.1016/j.echo.2009.11.018
21. Zhang Y, Zhou QC, Pu DR, Zou L, Tan Y. Differences in left ventricular twist related to age: Speckle tracking echocardiographic data for healthy volunteers from neonate to age 70 years. *Echocardiography*. 2010 Nov;27:1205-10. doi: 10.1111/j.1540-8175.2010.01226.x
22. Boissière J, Maufrais C, Baquet G, Schuster I, Dauzat M, Doucende G, et al. Specific left ventricular twist-untwist mechanics during exercise in children. J Am Soc Echocardiogr. 2013 Nov;26:1298-305. doi: 10.1016/j.echo.2013.07.007
23. Wang J, Khoury DS, Yue Y, Torre-Amione G, Nagueh SF. Left ventricular untwisting rate by speckle tracking echocardiography. *Circulation*. 2007 Nov 27;116(22):2580-6
24. Di Maria MV, Caracciolo G, Prashker S, Sengupta PP, Banerjee A. Left ventricular rotational mechanics before and after exercise in children. *J Am Soc Echocardiogr*. 2014 Dec;27:1336-43. doi: 10.1016/j.echo.2014.07.016

25. Homma Y, Hayabuchi Y, Terada T, Inoue M, Mori K. Early Diastolic Left Ventricular Relaxation in Normal Neonates is Influenced by Ventricular Stiffness and Longitudinal Systolic Function. *Int Heart J*. 2018 Jan 27;59:149-153. doi: 10.1536/ihj.17-125

Table 1. Demographic and Echographic data of the 43 newborns.

Variable	**First exam n=43**	**Second exam n=36**	***p-value***
Demographic data			
Gestational age (*weeks*)	39.9 ±1.0	NA	
Age (*days*)	3.4 ±0.8	78 ±7.6	
Female (*n*)	22 (51)	20 (55)	*0.6*
Body Weight (*kg*)	3.44 ±0.36	5.45 ±0.68	*<.001*
Body Height (*cm*)	51 ±2.3	59 ±2.4	*<.001*
OFC* (*cm*)	34.9 ±1.1	39.4 ±1.5	*<.001*
Echographic data			
Heart rate (*bpm*)	112 ±14.5	150 ±17.2	*<.001*
Cardiac Malformation	0	0	
Frame rate (Hz)			
Short-axis Basal Plane	109.30 ±9.20	90.30 ±9.80	*<.001*
Short-axis Apical Plane	110.00 ±9.30	89.80 ±11.10	*<.001*
LV length (*mm*)	30.70 ±2.20	37.00 ± 2.50	*<.001*

**OPC*: Occipital Frontal Circumference.

Continuous variables are expressed as mean±SD.

Categorical variables are expressed as counts (%).

Table 2. Left ventricle rotation and deformation parameters during postnatal adaptation

Parameter	First Exam (day 3-5) n=35	Second Exam (day 60-90) n=35	*p-value*
Primary endpoint			
LV Twist (°)	4.1 ±2.2	8.6 ±2.7	*<.001*
Secondary endpoints			
LV Torsion (°/cm)	1.3 ±0.7	2.3 ±0.8	*<.001*
Peak LV Twist rate (°/s)	41.4 ±20.4	81.3 ±29.4	*<.001*
Peak LV Untwist rate (°/s)	-48.5 ±23.0	-98.9 ±47.3	*<.001*
Basal Rotation (°)	-2.0 ±1.4	-5.6 ±1.3	*<.001*
Apical Rotation (°)	4.3 ±1.5	4.5 ±2.1	*0.63*
Basal Circumferential Strain (%)	-14.9 ±2.1	-18.9 ± 2.6	*<.001*
Apical Circumferential Strain (%)	-18.7 ±3.5	-17.6 ±4.1	*0.12*
Basal Radial Strain (%)	12.9 ±4.9	17.0 ±9.2	*0.015*
Apical Radial Strain (%)	14.7 ±4.6	27.6 ±11.1	*<.001*

Table 3. Comparison between Endocardial and Epicardial LV Circumferential Strain

Parameter	**Inner Layer (Endocardial) n=35**	**Outer Layer (Epicardial) n=35**	***p***
Basal Circumferential Strain (%) - First Exam	-18.24 ±2.65	-13.29 ±1.99	<.001
Basal Circumferential Strain (%) - Second Exam	-23.44 ±2.87	-16.65 ±2.77	<.001
Apical Circumferential Strain (%) - First Exam	-23.99 ±4.14	-16.29 ±3.30	<.001
Apical Circumferential Strain (%) - Second Exam	-24.76 ±5.58	-13.78 ±3.64	<.001

Table 4. Intraobserver and Interobserver variability measurements

Parameter	Intraobserver		Interobserver	
	ICC (95% IC)	**Bias (LOA)**	**ICC (95% CI)**	**Bias (LOA)**
Basal Circumferential Strain	0.94 (0.83 to 0.98)	0.13 (-2.42 to 2.68)	0.89 (0.67 to 0.96)	-1.19 (-4.19 to 1.82)
Apical Circumferential Strain	0.97 (0.91 to 0.99)	-0.94 (-3.53 to 1.65)	0.88 (0.65 to 0.96)	-3.93 (-8.26 to 0.40)
Basal Rotation	0.98 (0.94 to 0.99)	0.22 (-0.72 o 1.16)	0.96 (0.89 to 0.99)	-0.02 (-1.24 to 1.19)
Apical Rotation	0.97 (0.91 to 0.99)	0.16 (-0.65 to 0.96)	0.95 (0.85 to 0.98)	0.79 (-0.45 to 2.03)
Basal Peak Rotation Rate	0.99 (0.96 to 0.99)	0.57 (-8.14 to 9.28)	0.94 (0.81 to 0.98)	2.09 (-16.74 to 20.93)
Apical Peak Rotation Rate	0.98 (0.95 to 0.99)	0.73 (-8.05 to 9.51)	0.95 (0.86 to 0.98)	7.08 (-6.94 to 21.10)

ICC (95%IC), Intraclass Correlation Coefficient (95% Confidence Interval); *LOA*, limits of agreement

Figure legends

Figure 1. Left Ventricular Twist. Counterclockwise rotation of the apex and clockwise rotation of the base along the LV long axis when viewed from the apex.

Figure 2. 2D-STE Analysis. A, B. (*Patient 7; day 5*) Basal and Apical planes from parasternal short-axis views, respectively divided into 6 and 4 equal segments by the software. The myocardium is divided into two layers (Inner and Outer). **C.** (*Patient 42; day 3*) Basal plane from parasternal short-axis view with graphic representation of each segment rotation (color lines) and of global rotation (white line in bold). One cardiac cycle occurs between the two orange lines.

Figure 3. Box plot representation of LV rotation and deformation parameters at the first echocardiography (days 2-5) and at the second echography (days 60-90). Data are presented as medians, first and third quartiles, outliers (°) and means (x). n=35. * *when p<0.001*

Figure 4. Evolution of LV rotational mechanics parameters during postnatal adaptation. Values are presented as mean±2SD (bold line; dotted line) for Basal Rotation; Apical Rotation; LV Twist and LV Twist Rate.

Table 1. Demographic and Echographic data of the 43 newborns.

Variable	**First exam n=43**	**Second exam n=36**	***p-value***
Demographic data			
Gestational age (*weeks*)	39.9 ±1.0	NA	
Age (*days*)	3.4 ±0.8	78 ±7.6	
Female (*n*)	22 (51)	20 (55)	*0.6*
Body Weight (*kg*)	3.44 ±0.36	5.45 ±0.68	*<.001*
Body Height (*cm*)	51 ±2.3	59 ±2.4	*<.001*
OFC* (*cm*)	34.9 ±1.1	39.4 ±1.5	*<.001*
Echographic data			
Heart rate (*bpm*)	112 ±14.5	150 ±17.2	*<.001*
Cardiac Malformation	0	0	
Frame rate (Hz)			
Short-axis Basal Plane	109.30 ±9.20	90.30 ±9.80	*<.001*
Short-axis Apical Plane	110.00 ±9.30	89.80 ±11.10	*<.001*
LV length (*mm*)	30.70 ±2.20	37.00 ± 2.50	*<.001*

**OPC*: Occipital Frontal Circumference.

Continuous variables are expressed as mean±SD.

Categorical variables are expressed as counts (%).

Table 2

Table 2. Left ventricle rotation and deformation parameters during postnatal adaptation

Parameter	First Exam (day 3-5) n=35	Second Exam (day 60-90) n=35	*p-value*
Primary endpoint			
LV Twist (°)	4.1 ±2.2	8.6 ±2.7	*<.001*
Secondary endpoints			
LV Torsion (°/cm)	1.3 ±0.7	2.3 ±0.8	*<.001*
Peak LV Twist rate (°/s)	41.4 ±20.4	81.3 ±29.4	*<.001*
Peak LV Untwist rate (°/s)	-48.5 ±23.0	-98.9 ±47.3	*<.001*
Basal Rotation (°)	-2.0 ±1.4	-5.6 ±1.3	*<.001*
Apical Rotation (°)	4.3 ±1.5	4.5 ±2.1	*0.63*
Basal Circumferential Strain (%)	-14.9 ±2.1	-18.9 ± 2.6	*<.001*
Apical Circumferential Strain (%)	-18.7 ±3.5	-17.6 ±4.1	*0.12*
Basal Radial Strain (%)	12.9 ±4.9	17.0 ±9.2	*0.015*
Apical Radial Strain (%)	14.7 ±4.6	27.6 ±11.1	*<.001*

Table 3. Comparison between Endocardial and Epicardial LV Circumferential Strain

Parameter	**Inner Layer (Endocardial) n=35**	**Outer Layer (Epicardial) n=35**	***p***
Basal Circumferential Strain (%) - First Exam	-18.24 ±2.65	-13.29 ±1.99	<.001
Basal Circumferential Strain (%) - Second Exam	-23.44 ±2.87	-16.65 ±2.77	<.001
Apical Circumferential Strain (%) - First Exam	-23.99 ±4.14	-16.29 ±3.30	<.001
Apical Circumferential Strain (%) - Second Exam	-24.76 ±5.58	-13.78 ±3.64	<.001

Table 4. Intraobserver and Interobserver variability measurements

Parameter	Intraobserver		Interobserver	
	ICC (95% IC)	**Bias (LOA)**	**ICC (95% CI)**	**Bias (LOA)**
Basal Circumferential Strain	0.94 (0.83 to 0.98)	0.13 (-2.42 to 2.68)	0.89 (0.67 to 0.96)	-1.19 (-4.19 to 1.82)
Apical Circumferential Strain	0.97 (0.91 to 0.99)	-0.94 (-3.53 to 1.65)	0.88 (0.65 to 0.96)	-3.93 (-8.26 to 0.40)
Basal Rotation	0.98 (0.94 to 0.99)	0.22 (-0.72 o 1.16)	0.96 (0.89 to 0.99)	-0.02 (-1.24 to 1.19)
Apical Rotation	0.97 (0.91 to 0.99)	0.16 (-0.65 to 0.96)	0.95 (0.85 to 0.98)	0.79 (-0.45 to 2.03)
Basal Peak Rotation Rate	0.99 (0.96 to 0.99)	0.57 (-8.14 to 9.28)	0.94 (0.81 to 0.98)	2.09 (-16.74 to 20.93)
Apical Peak Rotation Rate	0.98 (0.95 to 0.99)	0.73 (-8.05 to 9.51)	0.95 (0.86 to 0.98)	7.08 (-6.94 to 21.10)

ICC (95%IC), Intraclass Correlation Coefficient (95% Confidence Interval); *LOA*, limits of agreement

Figure 1

Click here to download Figure Figure 1.tif

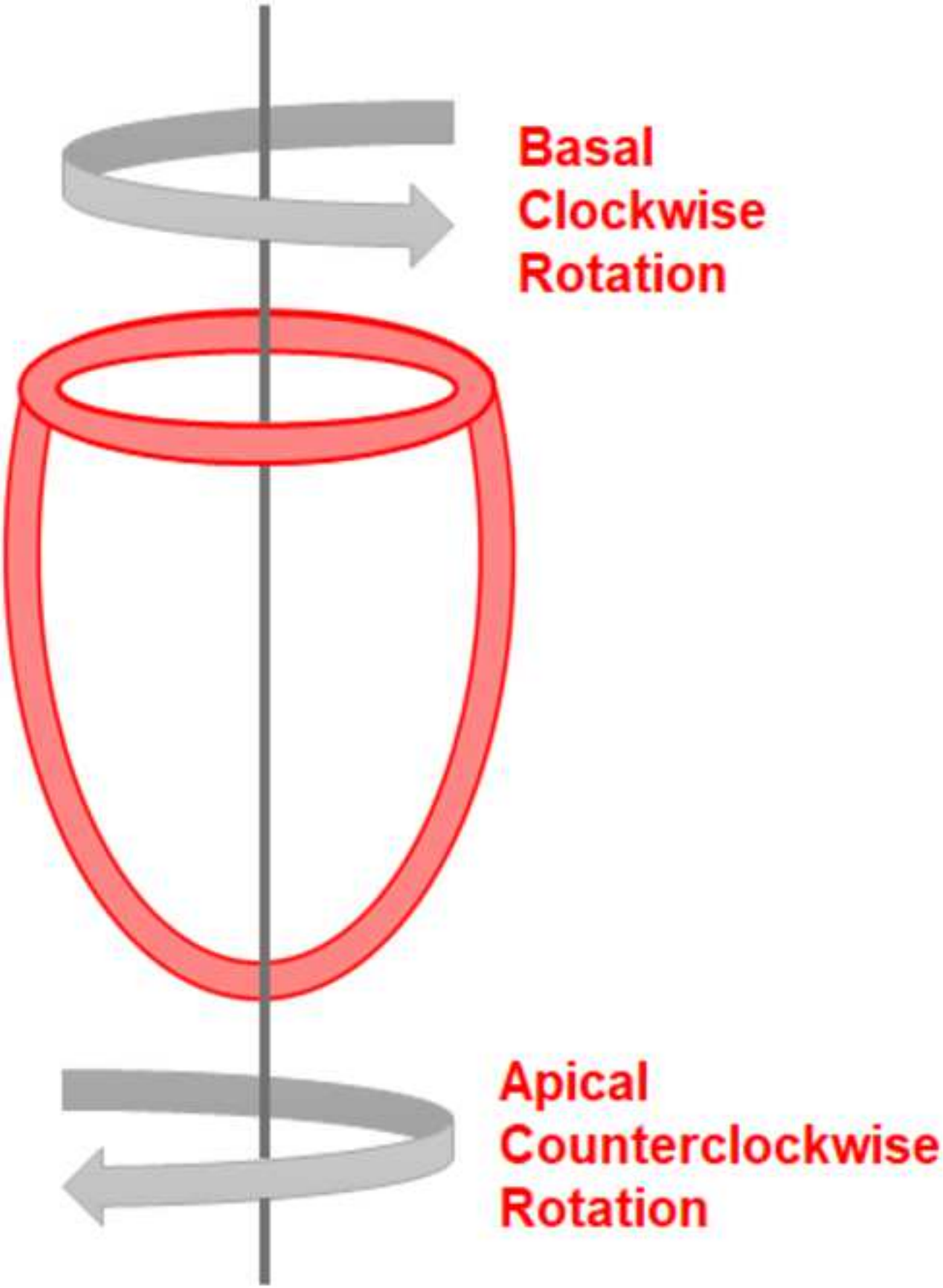

Figure 2

Click here to download Figure Figure 2.tif

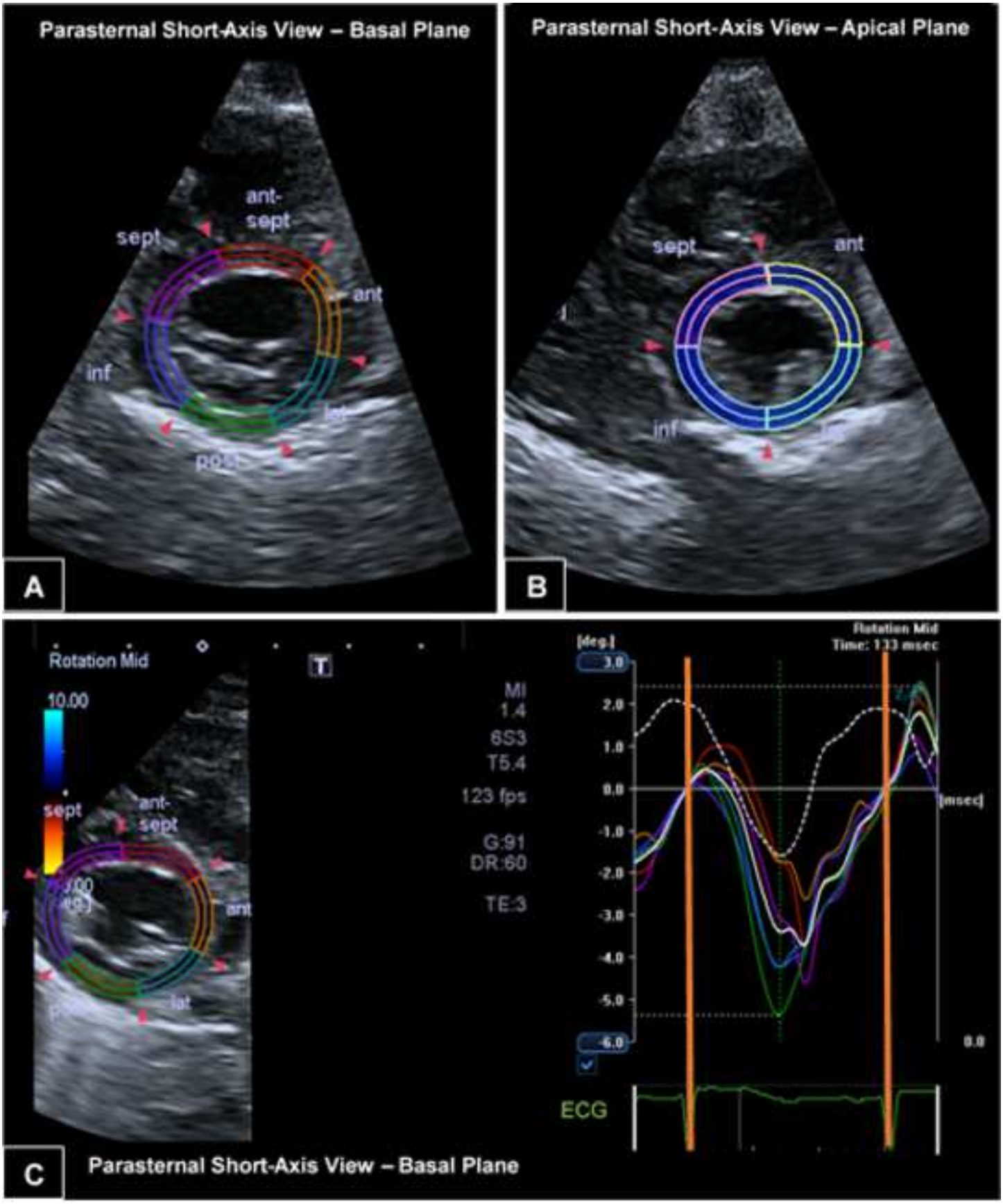

Figure 3

Click here to download Figure Figure 3.tif

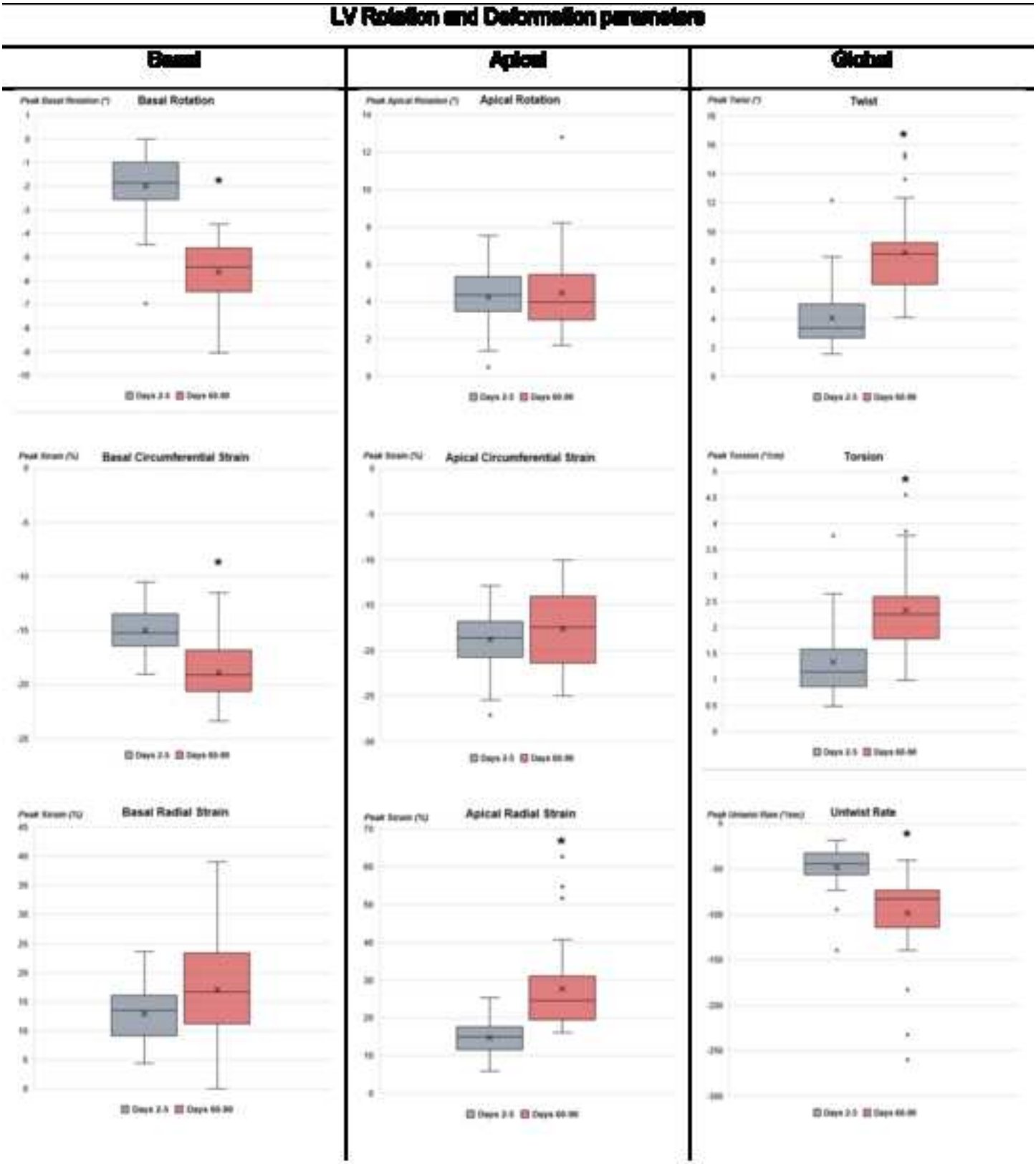

Figure 4

Click here to download Figure Figure 4.tif